View metadata, citation and similar papers at core.ac.uk

brought to you by CORE

provided by Institute of Cancer Research Repository

# Metabolic biomarkers of response to the AKT inhibitor MK-2206 in pre-clinical models of human colorectal and prostate carcinoma

N M S Al-Saffar[1*], H Troy[1†], A-C Wong Te Fong[1], R Paravati[1], L E Jackson[1], S Gowan[2], J K R Boult[1], S P Robinson[1], S A Eccles[2], T A Yap[3,4‡], M O Leach[1*] and Y-L Chung[1*]

[1]Cancer Research UK Cancer Imaging Centre, Division of Radiotherapy and Imaging. The Institute of Cancer Research and The Royal Marsden NHS Foundation Trust, London, SW7 3RP, United Kingdom. [2]Cancer Research UK Cancer Therapeutics Unit, Division of Cancer Therapeutics. The Institute of Cancer Research, London, SW7 3RP, United Kingdom. [3]Drug Development Unit, The Royal Marsden NHS Foundation Trust, London, SW7 3RP, United Kingdom. [4]Division of Clinical Studies, The Institute of Cancer Research, London, SW7 3RP, United Kingdom.

[*]Corresponding Authors:

Dr. Nada Al-Saffar

Cancer Research UK Cancer Imaging Centre, Division of Radiotherapy and Imaging

The Institute of Cancer Research and The Royal Marsden NHS Foundation Trust

123 Old Brompton Road, SW7 3RP, London, United Kingdom

Tel: +44 (0)20 8722 4686

Fax: +44 (0)20 8661 0846

Email: nada.al-saffar@icr.ac.uk

Prof. Martin Leach

Cancer Research UK Cancer Imaging Centre, Division of Radiotherapy and Imaging

The Institute of Cancer Research and The Royal Marsden NHS Foundation Trust

123 Old Brompton Road, SW7 3RP, London, United Kingdom

Tel: 020 8661 3338

Fax: 020 8661 0846

Email: Martin.Leach@icr.ac.uk

Dr. Yuen-Li Chung

Cancer Research UK Cancer Imaging Centre, Division of Radiotherapy and Imaging

The Institute of Cancer Research and The Royal Marsden NHS Foundation Trust

123 Old Brompton Road, SW7 3RP, London, United Kingdom

Tel: +44 (0)20 8722 4321

Fax: +44 (0)20 8661 0846

Email: Yuen-Li.Chung@icr.ac.uk

[†]Current address: Abbott Ireland Diagnostics Division, Pregnancy and Fertility Team, Lisnamuck, Longford, Ireland.

[‡]Current address: The University of Texas MD Anderson Cancer Center, Houston, TX, USA

Running title: Metabolic biomarkers of response to AKT inhibition

Key words: AKT, MRS, biomarkers, phospholipid metabolism.

**Abstract**

**Background:** AKT is commonly overexpressed in tumours and plays an important role in the metabolic reprogramming of cancer. We have used magnetic resonance spectroscopy (MRS) to assess whether inhibition of AKT signalling would result in metabolic changes that could potentially be used as biomarkers to monitor response to AKT inhibition.

**Methods:** Cellular and metabolic effects of the allosteric AKT inhibitor MK-2206 were investigated in HT29 colon and PC3 prostate cancer cells and xenografts using flow cytometry, immunoblotting, immunohistology and MRS.

**Results:** *In vitro* treatment with MK-2206 inhibited AKT signalling and resulted in time-dependent alterations in glucose, glutamine and phospholipid metabolism. *In vivo*, MK-2206 resulted in inhibition of AKT signalling and tumour growth compared with vehicle-treated controls. *In vivo* MRS analysis of HT29 subcutaneous xenografts showed similar metabolic changes to those seen *in vitro* including decreases in the tCho/water ratio, tumour bioenergetic metabolites and changes in glutamine and glutathione metabolism. Similar phosphocholine changes compared to *in vitro* were confirmed in the clinically relevant orthotopic PC3 model.

**Conclusion:** This MRS study suggests that choline metabolites detected in response to AKT inhibition are time- and microenvironment-dependent, and may have potential as non-invasive biomarkers for monitoring response to AKT inhibitors in selected cancer types.

## Background

The AKT/PKB (Protein Kinase B) serine/threonine kinase, with three different isoforms: AKT1, AKT2 and AKT3, is one of the core components of the PI3K signalling cascade, regulating cell proliferation, survival and metabolism, and is frequently activated in cancer (Manning and Toker, 2017). Multiple AKT inhibitors are now at various stages of clinical development (Brown and Banerji, 2017; Khan *et al*, 2013; Nitulescu *et al*, 2016). AKT inhibitors fall predominantly into two classes: ATP-competitive inhibitors and allosteric inhibitors of AKT (Brown and Banerji, 2017; Khan *et al*, 2013; Nitulescu *et al*, 2016). MK-2206 is a potent oral allosteric pan-AKT inhibitor with potential anti-neoplastic activity and is currently being evaluated in numerous clinical trials (Brown and Banerji, 2017; Khan *et al*, 2013; Nitulescu *et al*, 2016). Single-agent trials with this agent have generally shown anti-proliferative, rather than anti-tumour activity, with stable disease identified as the best overall response (Ahn *et al*, 2015; Yap *et al*, 2011; Yap *et al*, 2014). Therefore, identification of non-invasive biomarkers of target inhibition and potentially of tumour response would be of value in the clinical development of the AKT inhibitor MK-2206.

Reprogrammed metabolism is one of the hallmarks of cancer (Hanahan and Weinberg, 2011; Pavlova and Thompson, 2016). As many oncogenic signalling pathways that regulate cancer have also been shown to regulate metabolism (Iurlaro *et al*, 2014; Tarrado-Castellarnau *et al*, 2016), targeting those signalling pathways with drugs such as MK-2206 is expected to impact on metabolic intermediates. Assessment of the metabolic effects of drug treatment using functional imaging modalities, such as magnetic resonance spectroscopy (MRS) and metabolic PET, to provide an early

100 treatment response biomarkers to molecularly targeted drugs is being increasingly
101 investigated for clinical biomarker discovery (Beloueche-Babari *et al*, 2010;
102 Beloueche-Babari *et al*, 2011; Moestue *et al*, 2011; Serkova and Eckhardt, 2016;
103 Workman *et al*, 2006).
104
105 MRS provides a non-invasive and non-ionizing method of detecting various
106 tissue metabolites *in vitro*, *ex vivo* and *in vivo* (Gadian, 1995). Numerous studies have
107 investigated MRS-detectable metabolic biomarkers in response to novel targeted
108 therapies that are in pre-clinical development or early phase clinical evaluation
109 including inhibitors of HSP90, MAPK, HDAC, PI3K/AKT/mTOR and related
110 pathways, reviewed in (Beloueche-Babari *et al*, 2010; Beloueche-Babari *et al*, 2011;
111 Moestue *et al*, 2011).
112
113 Using MRS, we and others have previously reported alterations in the levels of
114 choline metabolites and/or lactate in response to different PI3K/mTOR pathway
115 inhibitors *in vitro* and *in vivo* in various cancer models (Al-Saffar *et al*, 2010; Al-
116 Saffar *et al*, 2014; Beloueche-Babari *et al*, 2006; Chaumeil *et al*, 2012; Esmaeili *et al*,
117 2014; Euceda *et al*, 2017; Koul *et al*, 2010; Lee *et al*, 2013; Moestue *et al*, 2013; Phyu
118 *et al*, 2016; Venkatesh *et al*, 2012). However to the best of our knowledge, metabolic
119 biomarkers for AKT inhibitors have only been evaluated *in vitro* and *ex vivo* in breast
120 cancer models (Moestue *et al*, 2013; Phyu *et al*, 2016; Su *et al*, 2012), and there are
121 no previous metabolic biomarker studies *in vivo* in tumour xenografts. In one study
122 (Su *et al*, 2012), treatment of MCF-7 and MDA-MB-231 breast cancer cells with the
123 alkylphospholipid AKT inhibitor perifosine resulted in decreases in PC and lactate
124 production. Two studies reported different results using the allosteric AKT inhibitor

MK-2206, which provides greater specificity, reduced side-effects and less toxicity compared to alkylphospholipid AKT inhibitors (Nitulescu *et al*, 2016). A decrease in PC levels was observed *in vitro* in MDA-MB-468 breast cancer cells (Phyu *et al*, 2016), while an increase in PC and a decrease in lactate levels were detected *ex vivo* in basal-like breast cancer tumours following treatment with MK-2206 (Moestue *et al*, 2013).

In view of the inconsistent published findings with the allosteric AKT inhibitor MK-2206, and the lack of *in vivo* studies in cancer models, we set out to assess the metabolic changes in response to MK-2206 both *in vitro* and *in vivo* in subcutaneous and orthotopic animal xenograft models of colon and prostate cancer, with potential to develop these metabolic changes as non-invasive biomarkers for monitoring response in clinical trials.

Our results show that treatment with the AKT inhibitor MK-2206 results in metabolic changes detectable with MRS. Importantly, a decrease in the total choline (tCho)/water ratio was observed in the more clinically relevant orthotopic model of the PC3 prostate cancer and therefore may provide a potential non-invasive biomarker for monitoring response to MK-2206 during clinical trials.

## Materials and Methods

**Cell culture and treatment.** The human PTEN null PC3 prostate adenocarcinoma and *PIK3CA* mutant HT29 colorectal carcinoma cell lines (American Type Culture Collection) were cultured in DMEM (Life Technologies) supplemented with 10% fetal calf serum (PAA labs Ltd), 100 U/mL penicillin, and 100 μg/mL streptomycin (Life Technologies) at 37°C in 5% $CO_2$. Cell viability was routinely >90%, as judged by trypan blue exclusion. All cell lines were shown to be mycoplasma free using a PCR-based assay (Surrey Diagnostics Ltd) and were authenticated in our laboratory by short tandem repeat (STR) profiling.

Both cell lines were treated with the orally active, highly selective non-ATP competitive allosteric AKT inhibitor MK-2206 (Merck & Co., Inc.). $GI_{50}$ values (concentrations causing 50% inhibition of proliferation for tumour cells) were determined using the sulforhodamine B assay following 96 h continuous exposure to compounds (Raynaud *et al*, 2007). At the required time points, cells underwent trypsinization and trypan blue exclusion assay (Al-Saffar *et al*, 2014). The effect of treatment on cell number was monitored by counting the number of viable attached cells in a treated flask and comparing that number with the number of attached cells in a control flask.

**Flow cytometry**. Cell cycle analysis was performed as previously described (Al-Saffar *et al*, 2014).

**Immunoblotting.** Western blotting was performed as previously described (Al-Saffar *et al*, 2014). Western blots were probed for pAKT (Ser473; 4060), AKT (9272),

pRPS6 (Ser240/244; 2215), RPS6 (2217), HK2 (2106), PARP (9542), LDHA (3582), β-Actin (4967), all from Cell Signaling Technology, and CHKA (HPA0241153) from Sigma. Blots were revealed with peroxidase-conjugated secondary anti-rabbit (GE Healthcare NA9340) or anti-mouse (DAKO P0260) antibodies followed by ECL chemiluminescence solution (Amersham Biosciences).

***In vitro* $^{1}$H- and $^{31}$P-MRS of cell extracts.** The same number of cells per flask were seeded at the beginning of the experiment then at the selected time points; cells were pooled from the number of flasks required to achieve an average cell number of $3x10^{7}$ cells, which differed depending on the expected effect of treatments on cell number. To obtain an MR spectrum, cells were extracted from cultured cells using the dual phase extraction method, as previously described (Al-Saffar *et al*, 2014; Tyagi *et al*, 1996). Briefly, cells were rinsed with ice-cold saline and fixed with 10 mL of ice-cold methanol. Cells were then scraped off the surface of the culture flask and collected into tubes. Ice-cold chloroform (10 mL) was then added to each tube followed by an equal volume of ice-cold deionized water. Following phase separation, the solvent in the upper methanol/water phase was removed by lyophilisation. Prior to acquisition of the MRS spectra, the water-soluble metabolites were resuspended in deuterium oxide ($D_2O$) for $^{1}$H-MRS or $D_2O$ with 10 mM EDTA (pH 8.2) for $^{31}$P-MRS. For extracellular metabolite analysis, 500 µL of cell growth medium was mixed with 100 µL of D2O containing sodium 3-trimethylsilyl-2,2,3,3-tetradeuteropropionate as an internal reference (TSP; 2.7 mM). $^{1}$H-MRS and $^{1}$H-decoupled $^{31}$P-MRS spectra were acquired at 25°C on a 500 MHz Bruker spectrometer (Bruker Biospin, Coventry, UK) using a 90-degree flip angle, a 1 s relaxation delay, spectral width of 12 ppm, 64 K data points, and HDO resonance suppression by presaturation for $^{1}$H-MRS and a 30°

flip angle, a 1 s relaxation delay, spectral width of 100 ppm, and 32 K data points for $^{31}$P. Metabolite contents were determined by integration and normalised relative to the peak integral of an internal reference [TSP (4.8 mM) for $^{1}$H-MRS, and methylenediphosphonic acid (MDPA; 2 mM) for $^{31}$P-MRS] and corrected for signal intensity saturation ($^{31}$P-MRS) and the number of cells extracted per sample.

***In vivo* tumour propagation.** All animal experiments were performed in accordance with local and national ethical review panel, the UK Home Office Animals (Scientific Procedures) Act 1986 and the United Kingdom Coordinating Committee on Cancer Research Guidelines for the Welfare of Animals in Experimental Neoplasia (Workman *et al*, 2010).

**Subcutaneous HT29 and PC3 tumour xenografts.** Male NCr nude mice were injected subcutaneously in the flank with $5x10^6$ HT29 (human colon) or PC3 (human prostate) carcinoma cells. Tumour volume was calculated by measuring the length, width, and depth using calipers and the ellipsoid formula L x W x D x ($\pi$/6). Once the tumours reached ~400 mm$^3$, the animals were divided to two groups. One group was treated with 2 doses of 120 mg/kg of MK-2206 on alternate days (Day 1 and 3) via p.o. and the other group with vehicle alone (10% DMSO in saline).

**Orthotopic PC3 tumour xenografts.** PC3 cells ($5 \times 10^5$) were inoculated in the ventral prostate gland of nude mice. Once the tumours were palpable, animals were treated with 2 doses of 120 mg/kg of MK-2206 on alternate days (Day 1 and 3) via p.o. or vehicle alone (10% DMSO in saline).

***In vivo* MRS of HT29 and PC3 tumours.** Mice were anesthetised with a single intraperitoneal injection of a fentanyl citrate (0.315 mg/mL) plus fluanisone [10 mg/mL (Hypnorm; Janssen Pharmaceutical Ltd., High Wycombe, UK)], midazolam [5 mg/mL (Hypnovel; Roche, Welwyn Garden City, UK)], and sterile water (1:1:2) at a dose of 9 mL/kg. They were placed in the bore of a 7 Tesla Bruker MR System spectrometer (Bruker Biospin, Coventry, United Kingdom) with HT29 and PC3 tumours positioned in the centre of a 15 mm two-turn $^{1}H/^{31}P$ surface coil. *In vivo* localised PRESS $^{1}H$-MRS of the tumours was carried out at 37°C on Day 0 (before treatment) and the last day of treatment (Day 3). 4 mm x 4 mm x4 mm voxels were selected from fast spin-echo images and shimmed using a localised sequence. The localised PRESS with water suppression was used to detect choline with a repetition time of 4 s, echo times 136 ms and 64 transients. 4 transients were used to acquire the unsuppressed water spectra with the same acquisition parameters as above. Image-selected *in vivo* spectroscopy (ISIS) $^{31}P$-MR spectra were also obtained in subcutaneous PC3 tumours with a repetition time of 2 s and 64 transients. After the final MRS scan, tumours were excised and stored at for subsequent *ex vivo* $^{1}H$- and $^{31}P$-MRS, MSD® assays or immunohistochemical analysis.

$^{1}H$- and $^{31}P$-MR spectra were analysed using the JMRUI programme to pre-process, fit and quantify peak areas of the observed metabolites. Choline levels are expressed as a ratio relative to the water (tCho/water) signal following corrections for the number of averages and receiver gains, as these two parameters were different for the acquisitions of water and choline spectra. Phosphomonoesters (PMEs) were expressed as ratios relative to total phosphorus (PMEs/total P) signals.

**Meso Scale Discovery (MSD®) assay.** Tumour pharmacodynamic biomarkers for MK-2206 were assessed by a MSD® multispot electrochemiluminescence immunoassay system to detect pP70S6K (Thr421/Ser424), total P70S6K, pAKT (Ser473), pAKT (Thr308), total AKT, pRPS6 (Ser235/236), pRPS6 (Ser240/244) and total RPS6 in 10 mg tumour lysate of vehicle and MK-2206 treated tumours according to the manufacturer's instructions (Meso Scale Discovery, Gaithersburg, USA).

***Ex vivo* MRS of tumour extracts.** 100- 200 mg of the freeze-clamped tumours were finely grinded in liquid nitrogen and extracted using ice-cold methanol, water and chloroform (1:1:1). The aqueous phase was separated, freeze-dried and reconstituted in 650 µl $D_2O$. 50 µL of 44 mM TSP in $D_2O$ was added to the samples for $^1H$ chemical shift calibration and quantification. The samples were then placed in 5 mm NMR tubes and sample pH was adjusted to 7 using perchloric acid or potassium hydroxide. $^1H$-MRS of the tumour extracts was performed on a Bruker 500 MHz nuclear magnetic resonance system (Bruker Biospin, Coventry, United Kingdom) and spectra were acquired using a pulse and collect NMR sequence with presaturation for water suppression; 7500 Hz spectral width, 32 K time domain points, 2.7 s relaxation delay and 256 scans at 298 K. After $^1H$-MRS, 50 µL of 60 mM EDTA was added to each sample for chelation of metal ions and 25 µL of 10 mM MDPA was added to the samples for $^{31}P$ chemical shift calibration and quantitation. The pH was again adjusted to 7 and $^{31}P$-MRS was performed with 12000 Hz spectral width, 32K time domain points, 5 s relaxation delay and 3000 scans at 298 K (Chung, 2017).

MR spectra were analysed using the Bruker Topspin-3.2 software package (Bruker Biospin, Coventry, UK). Spectra were processed by using exponential multiplication with a line broadening of 0.3 Hz and 3 Hz for $^{1}$H- and $^{31}$P-MR spectra, respectively, then followed by Fourier transform, zero- and first-order phase correction, baseline correction and spectral peak integration integration. Spectral assignments were based on literature values (Chung, 2017; Sitter *et al*, 2002). Water-soluble metabolites measured by $^{1}$H and $^{31}$P-MRS were quantified relative to TSP or MDPA, respectively, and standardised to tumour weight (Chung, 2017).

**Immunohistochemistry.** Tumour xenografts were fixed in 10% formaldehyde and routinely processed for paraffin embedding. For histological evaluation, 5 μm-thick paraffin wax sections were cut and stained with haematoxylin and eosin (H&E). Expression of caspase-3 (apoptotic marker), CD31 (micro-vessel density) and Ki67 (proliferation marker) were determined by immunohistochemistry, using the streptavidin-biotin peroxidase technique. Briefly, sections of 5 μm were deparaffinised in xylene and rehydrated through graded ethanol concentrations up to distilled water for 30 min. Antigen retrieval was performed by microwaving the sections in 10 mM sodium citrate buffer pH 6 at 10 min intervals for a total of 20 min and cooling for 1 h at room temperature (RT). Endogenous peroxidase activity was blocked by incubating the sections in a solution of 3% hydrogen peroxide for 20 min at RT. After washing in PBS (phosphate buffer saline), sections were incubated with the primary polyclonal rabbit anti-human caspase-3 (1:50, Abcam ab2302), monoclonal rabbit anti-human CD31 (1:50, Millipore 04-1074) mouse monoclonal anti-human Ki67 (1:75, DAKO M7240) antibodies, overnight at 4°C. The sections were washed with PBS and incubated with a biotinylated secondary antibody for 45

min, followed by an incubation with streptavidin-biotin horseradish peroxidase complex (DAKO) for another 45 min, at RT. Staining was carried out using a solution 3,3'-diaminobenzidine (DAB-Sigma), and lightly counterstained with Harris haematoxylin.

**Evaluation of staining.** Sections known to express high levels of caspase-3 (pancreas), CD31 (liver) and Ki67 (tonsil) were included as positive controls, while negative control slides were incubated with PBS. Caspase-3 and Ki67 immuno-stained slides were assessed by light microscopy and scored with ImageJ (1.50i). A semi-quantitative method was used to score the microvessels stained with CD31 (Bosari *et al*, 1992). Three fields showing the highest number of microvessels were selected using light microscopy and the number of micovessels in these fields were then manually counted and averaged. Each section was scored by 2 independent observers at x200 magnification.

**Statistical analysis.** Data are presented as the mean ± SD (*in vitro*) or mean ± SEM (*in vivo* and *ex vivo*) and $n \geq 3$. Statistical significance of differences was determined by Student's standard t-tests with a $P$ value of $\leq 0.05$ considered to be statistically significant.

## Results

***In vitro* investigation of molecular and metabolic effects of treatment with MK-2206 in PC3 human prostate cancer cells.** The PTEN null human prostate cell line PC3 was treated with MK-2206 for 6, 12 and 24 h at a pharmacologically active concentration corresponding to 5x$GI_{50}$ ($GI_{50}$ = 5 μM). Inhibition of the AKT pathway was evident at all time points as indicated by decreased phosphorylation of AKT (Ser473) and RPS6 (Ser240/244) in treated cells compared to their controls (Figure 1A). Treatment with MK-2206 also induced apoptosis which was evident at 12 and 24 h following treatment as indicated by PARP cleavage detected by immunoblotting (Fig 1A). Inhibition of cell growth (down to 66 ± 10%, $P$ = 0.0001) and a G1 cell cycle arrest was only detectable at 24 h post treatment (Figure 1B).

$^{31}$P-and $^{1}$H-MRS of aqueous extracts from PC3 cells treated *in vitro* with the AKT inhibitor MK-2206 (5x$GI_{50}$) was used to identify potential biomarkers of AKT pathway inhibition compared to controls (Figure 1C). Analysis of metabolites detected with $^{31}$P-MRS showed a significant decrease ($P \leq 0.02$) in the levels of phosphoethanolamine (PE), phosphocholine (PC) and NTP which was evident at 6 h and was maintained at 24 h (Table 1). Levels of glycerophosphoethanolamine (GPE) and glycerophosphocholine (GPC) were reduced for up to 12 h ($P \leq 0.001$) but then a significant increase ($P \leq 0.01$) was observed at 24 h (Table 1). A significant decrease ($P \leq 0.04$) in the levels of phosphocreatine (PCr) was also detected at 12 h and was maintained at 24 h following treatment with MK-2206. $^{1}$H-MRS confirmed changes in PC and GPC detected with $^{31}$P-MRS together resulted in a significant decrease ($P \leq 0.04$) in tCho levels (Figure 1D). Furthermore, significant decreases ($P \leq 0.05$) in lactate, alanine, glutamine, glutathione, creatine (Cr) and PCr levels were detected

over the time course of treatment (Figure 1E). A significant ($P \leq 0.05$) decrease in glutamate and increase in glucose were also found following 24 h of MK-2206 treatment (Figure 1E). We also assessed the metabolic effects of MK-2206 at a lower concentration equivalent to $3xGI_{50}$ for 24 h. This resulted in inhibition of AKT signalling and cellular growth (down to 84 ± 8%, $P = 0.008$) as well as a G1 cell cycle arrest compared to controls, but did not induce apoptosis as detemined by cleaved PARP (Supplementary Figure S1A). $^{31}$P-MRS showed similar changes in PC, PE, PCr and NTP to those observed with MK-2206 at $5xGI_{50}$, but levels of GPE and GPC were not affected (Table 1). Similarly, decreases in PC, tCho, lactate, alanine, glutathione, Cr and PCr were detected using $^{1}$H-MRS, while glutamate, glutamine and glucose levels remained unchanged relative to controls (Supplementary Figure S1B and C).

***In vitro* investigation of molecular and metabolic effects of treatment with MK-2206 in HT29 human colon cancer cells.** To test for the generality of the MRS-detected data, we also treated *PIK3CA* mutant HT29 colorectal carcinoma cells with MK-2206 at $5xGI_{50}$ ($GI_{50}$ = 0.4 μM) for 24 h. Similar to PC3 prostate cells, treatment with MK-2206 resulted in inhibition of AKT signalling and a G1 cell cycle arrest but no effects on cell number nor apoptosis were detected relative to controls (Supplementary Figure S2A and B). Representative $^{31}$P- and $^{1}$H-MR spectra are shown in Supplementary Figure S2C. As in PC3 cells, $^{31}$P-MRS analysis showed significant decreases ($P \leq 0.04$) in PE, PC, PCr and NTP and increases in GPE and GPC in spectra from MK-2206 treated cells compared to their controls (Table 1). $^{1}$H-MRS confirmed changes in PC, GPC and further showed a reduction in tCho (Supplementary Figure S2D). Consistent with PC3 cells, significant decreases ($P \leq$

362 0.04) in lactate, alanine, glutamate, glutamine, glutathione, Cr and PCr were also
363 observed in HT29 cells following MK-2206 treatment (Supplementary Figure S2E).
364 In contrast to PC3 cells, treatment with MK-2206 reduced glucose levels in HT29
365 cells ($P < 0.02$; Supplementary Figure S2E).
366
367 **Assessment of mechanisms underlying the *in vitro* MRS detected metabolic**
368 **changes following treatment with MK-2206**. We have used immunoblotting to
369 identify the effects of AKT inhibition with MK-2206 on enzymes involved in choline
370 and glucose metabolism. A decrease in choline kinase alpha (CHKA) expression
371 levels compared to control cells was observed over the time course of treatment with
372 MK-2206 in PC3 and following 24 h treatment with MK-2206 in HT29 cells
373 (Supplementary Figure S3A and B). For the glycolytic metabolic changes, reductions
374 in the protein expression levels of the glycolytic enzymes including hexokinase II
375 (HK2) and lactate dehydrogenase alpha (LDHA) were detected in both cell lines
376 following treatment with MK-2206 (Supplementary Figure S3A and B).
377
378 Next, in order to determine whether the changes in intracellular metabolites
379 could be due to alterations in metabolic flux, we used $^{1}$H-MRS to measure levels of
380 metabolites in the growth media of control and treated cells. In the PC3 cells
381 (Supplementary Figure S4A), treatment with MK-2206 ($5xGI_{50}$) caused no significant
382 changes in external metabolites at 6 h compared to controls. However, significant
383 increases ($P < 0.05$) in the levels of alanine, glutamine and choline were observed at
384 12 h following treatment. High levels of all metabolites were detected in growth
385 media of 24 h treated cells compared to controls resulting from the release of
386 metabolites from fragmented apoptotic cells. In contrast, 24 h treatment with MK-

2206 at $3xGI_{50}$ only caused a significant increase ($P = 0.01$) in the level of choline compared to controls. Increases in the levels of metabolites present in the growth media from HT29 cells treated with MK-2206 ($5xGI_{50}$) were detected but did not reach significance relative to controls (Supplementary Figure S4B).

***In vivo* investigation of molecular and metabolic effects of treatment with MK-2206 in subcutaneous HT29 colon xenografts.** Significant tumour growth inhibition was observed in HT29 xenografts after 2 doses (Day 1 and 3) of MK-2206 (120 mg/kg per dose) when compared with vehicle-treated controls (Figure 2A). AKT inhibition was confirmed by reductions in the phosphorylation of P70S6K, RPS6 (Ser235/236), AKT (Ser473) and AKT (Thr308; Supplementary Figure S5). *In vivo* $^{1}$H-MRS showed a significant decrease ($P = 0.04$) in the ratio of tCho/water signal in HT29 xenografts after MK-2206 treatment (Table 2). The *in vivo* change in tCho/water was confirmed by lower PC, GPC and GPE levels in *ex vivo* $^{31}$P-MRS analysis of MK-2206 treated tumour extracts when compared with vehicle controls (Table 2). Lower levels of glutamine, glutamate, aspartate, glycine, glutathione and Cr were also seen in MK-2206 treated tumours when compared with controls (Table 2). Phosphocreatine, ATP+ADP, NTP [0.68 ± 0.07 (control) versus 0.48 ± 0.03 (MK-2206) μmol/g wet weight; $P = 0.015$] and NDP [0.49 ± 0.02 (control) versus 0.30 ± 0.02 (MK-2206) μmol/g wet weight; $P = 0.0004$] levels were also found to reduce in the MK-2206 treated group (Table 2). No change in glucose and lactate levels, microvessel density, necrosis, proliferation or apoptosis was found in MK-2206 treated HT29 tumours when compared to vehicle controls using immunohistochemistry.

***In vivo* investigation of molecular and metabolic effects of treatment with MK-2206 in subcutaneous PC3 prostate tumour xenografts.** Similar to MK-2206 treated HT29 xenografts, significant tumour growth inhibition was also observed in PC3 xenografts after 2 doses (Day 1 and 3) of MK-2206 (120 mg/kg per dose) when compared with vehicle-treated controls (Figure 2B) and AKT inhibition was confirmed by the reductions in the phosphorylation of P70S6K, RPS6 (Ser235/236), AKT (Ser473) and AKT (Thr308) (Supplementary Figure S6). *In vivo* $^{1}$H-MRS did not show a change in the ratio of tCho/water signal in either control or MK-2206 treated PC3 xenografts (Table 3). However, a significant increase ($P$ = 0.02) in the ratio of PMEs/total P signal was found in MK-2206 treated PC3 xenografts by *in vivo* $^{31}$P-MRS (Table 3), with this *in vivo* change attributable to a significant increase ($P$ = 0.03) in PE measured by $^{31}$P-MRS of MK-2206 treated PC3 tumour extracts (Table 3). Significant decreases ($P \leq 0.04$) in GPC, GPE and lactate and increase in glutamine were also found in MK-2206 treated PC3 tumour extracts when compared with vehicle controls (Table 3). No change in tumour bioenergetics was observed in this tumour model following MK-2206 treatment. Immunohistochemical analysis (Figure 2C) on the tumour samples showed significantly decreased microvessel density (CD31) in MK-2206 treated tumours (9 ± 2 stained blood vessels average over 3 fields) when compared to vehicle-controls (14 ± 2; $P$ = 0.05). Using immunohistochemistry, no change in necrosis, proliferation or apoptosis was found in MK-2206 treated tumours when compared to controls (Figure 2C).

***In vivo* investigation of molecular and metabolic effects of treatment with MK-2206 in orthotopic PC3 prostate xenografts.** Next we wanted to examine the metabolic response to MK-2206 in a more clinically relevant *in vivo* model.

Orthotopic PC3 tumours were propagated, treated with MK-2206 (2 doses of 120 mg/kg on Day 1 and 3) and studied by $^{1}$H-MRS. AKT inhibition was confirmed by the reductions in phosphorylated RPS6 (Ser240/244), AKT (Ser473) and AKT (Thr308; Supplementary Figure S7). *In vivo* $^{1}$H-MRS showed that the tCho/water ratio was significantly reduced ($P = 0.02$) in orthotopic PC3 tumours after MK-2206 treatment, with this reduction attributable to a significant decrease ($P = 0.003$) in PC as measured *ex vivo* by $^{31}$P-MRS analysis of the tumour extracts (Table 4). Significant decreases ($P \leq 0.03$) in alanine and increases in glucose were also found in MK-2206 treated tumours (Table 4). No changes in tumour bioenergetics, glutamine or glutathione metabolism were observed in this tumour model following MK-2206 treatment. No change in microvessel density, necrosis, proliferation or apoptosis was found in MK-2206 treated tumours when compared to vehicle-controls.

## Discussion

AKT is a central component of the PI3K signalling pathway, influencing multiple processes that are directly involved in tumorigenesis. Targeting AKT is therefore a highly attractive anti-cancer strategy and several AKT inhibitors are currently in different phases of clinical trials (Brown and Banerji, 2017; Khan *et al*, 2013; Nitulescu *et al*, 2016). As with most cancer targeted therapy, AKT inhibitors were shown to cause anti-proliferative, rather than anti-tumour activity, with stable disease identified as the best overall response (Ahn *et al*, 2015; Yap *et al*, 2011; Yap *et al*, 2014). Therefore, the use of conventional, anatomically based end-points such as RECIST is inadequate (Serkova and Eckhardt, 2016; Teng *et al*, 2013). AKT also plays a pivotal role in the metabolic reprogramming of cancer, providing a rationale for the use of non-invasive functional imaging techniques (such as MRS or PET) as alternative methods to monitor response to this targeted therapy (Beloueche-Babari *et al*, 2010; Beloueche-Babari *et al*, 2011; Moestue *et al*, 2011; Serkova and Eckhardt, 2016; Workman *et al*, 2006).

We used MRS both *in vitro* and *in vivo* to identify whether inhibition of AKT signalling using the allosteric pan-AKT inhibitor MK-2206 would result in metabolic changes that can potentially be used to monitor response to AKT inhibition in clinical trials. We performed our investigation using the human *PIK3CA* mutant colorectal carcinoma HT29 and PTEN null prostate carcinoma PC3 cancer models as AKT signalling is involved in the tumorigenesis of colorectal and prostate cancers and AKT inhibitors are in clinical evaluation for both cancer types (Agarwal *et al*, 2013; Toren and Zoubeidi, 2014; Yap *et al*, 2016).

MK-2206 consistently resulted in the reduction of AKT and its downstream, mTOR, signalling pathways in PC3 and HT29 cells and tumours confirming the mechanism of action.

Treatment of PC3 cells with MK-2206 resulted in decreases in PE, PC, tCho, lactate, alanine, glutamine, glutathione, Cr, PCr and NTP levels from 6 h post-treatment onwards which was associated with AKT/mTOR pathway inhibition, but was much earlier than the G1 arrest, induction of apoptosis and the decrease in proliferation which were only evident at 24 h following treatment with MK-2206. This indicates that our detected metabolic changes are related to the inhibition of AKT/mTOR signalling rather than to the anti-proliferative effects of the treatment. In support of previous reports by ourselves and others using PI3K/mTOR/AKT inhibitors (Al-Saffar *et al*, 2010; Al-Saffar *et al*, 2014; Chaumeil *et al*, 2012; Su *et al*, 2012; Venkatesh *et al*, 2012), the decrease in PC levels following MK-2206 treatment was associated with a decrease in the protein levels of CHKA, the enzyme responsible for choline phosphorylation to form PC. A decrease in the protein expression levels of the glycolytic enzymes HK2 and LDHA were also observed following AKT inhibition, suggesting mechanisms for the depletion of lactate. Higher levels of choline were also found in the tissue culture media of cells treated with MK-2206 compared to controls indicating inhibition of uptake as another mechanism for the decrease in intracellular levels of PC. Furthermore, decreased intracellular and increased extracellular levels of alanine indicate the conversion of pyruvate into alanine instead of lactate as a result of inhibition of LDHA and increased eflux of alanine following treatment with MK-2206. A decrease in the intracellular and increase in the extracellular level of glutamine was also detected in treated cells which

maybe related to decreased uptake of glutamine into the cells following MK-2206 treatment.

Treatment with MK-2206 also reduced levels of GPE and GPC for up to 12 h but then an increase was observed at 24 h. The later increase in GPE and GPC might be linked to the apoptotic effects of MK-2206 observed at this time point which would lead to membrane breakdown and remodeling (Morse *et al*, 2007; Zhang *et al*, 2018). We have previously observed an increase in GPC following treatment with some PI3K inhibitors but that was cell line dependent and, moreover, was seen only after longer inhibition periods (≥ 16 h) and when higher concentrations ($5xGI_{50}$) of PI3K pathway inhibitors were used (Al-Saffar *et al*, 2010; Al-Saffar *et al*, 2014; Beloueche-Babari *et al*, 2006). This was further supported by our findings that when we used MK-2206 at a concentration equivalent to $3xGI_{50}$. This concentration did not cause apoptosis and had no effects on GPC or GPE levels.

Similar to PC3 cells, metabolic changes including reductions in PE, PC, tCho, lactate, alanine, glutamate, glutamine, glutathione, Cr and PCr as well as an increase in GPE and GPC were detected following treatment of HT29 colorectal carcinoma cells with MK-2206 at $5xGI_{50}$ for 24 h. This was associated with inhibition of AKT/mTOR signalling and a G1 cell cycle arrest. The observed changes in phospholipid and glucose metabolism are congruent with the previous reports examining the effect of the AKT inhibitors perifosine and MK-2206 on breast cancer cells (Phyu *et al*, 2016; Su *et al*, 2012), and suggest that choline-containing metabolites and lactate may serve as non-invasive metabolic biomarkers for monitoring the effects of AKT inhibitors.

Similar phospholipid and glutamine changes to those detected in HT29 cells were also observed in HT29 xenografts following treatment with MK-2206. These were associated with a significant tumour growth delay and pathway inhibition when compared with vehicle-treated controls. *In vivo* $^{1}$H-MRS analysis of the HT29 tumour xenografts showed a significant decrease in the ratio of tCho/water signal. This was further confirmed by significantly lower PC, GPC and GPE levels by *ex vivo* $^{31}$P-MRS of MK-2206 treated tumour extracts when compared with vehicle controls, supporting the *in vitro* findings and suggesting that membrane turnover is reduced following MK-2206 treatment. Tumour bioenergetics was also compromised by treatment with MK-2206 as indicated by the decrease in the levels of PCr, ATP+ADP, NTP and NDP. Consistent with our *in vitro* cell data, alterations in glutamine and glutathione metabolism with decreased glutamine, glutamate, aspartate, glutathione, glycine and Cr were also found in HT29 tumours following AKT inhibition with MK-2206. No change in glucose metabolism was observed in MK-2206 treated HT29 xenografts.

Glutamine is one of the key substrates utilised by cancer cells and its metabolism is important to tumour growth, malignancy, and survival under stress (Hensley *et al*, 2013). Glutamine is involved in nucleotide synthesis (Cory and Cory, 2006), and generation of the anti-oxidant glutathione (Shanware *et al*, 2011). The decreases in bioenergetic metabolites, such as nucleotides and PCr following MK-2206 treatment are consistent with the observed decreases in glycine, glutamine and its downstream metabolites, such as glutamate, aspartate and Cr, suggesting that lower

549 tumour bioenergetics following treatment maybe a consequence of changes in
550 glutamine metabolism.
551
552 Our data also indicate that glutathione biosynthesis may be altered following
553 MK-2206 treatment, as the total glutathione level together with its precursors,
554 glutamine and glycine, were lower in the MK-2206 treated PC3 and HT29 cells and
555 tumours. This is consistent with previous reports that glutathione levels are reduced in
556 MK-2206 treated lung cancer cells (Dai *et al*, 2013) and that the PI3K/AKT signalling
557 pathway in *PIK3CA* mutant and *PTEN* mutant breast cancer cells stimulates
558 glutathione biosynthesis, in order to counteract the effect of oxidative stress (Lien *et*
559 *al*, 2016).
560
561 Different changes in PC levels have been previously reported following
562 treatment with MK-2206 in MDA-MB-468 breast cancer cells (Phyu *et al*, 2016)
563 compared to basal like breast cancer tumours (Moestue *et al*, 2013). This was the case
564 with MK-2206 treated subcutaneous PC3 xenografts, where in contrast to PC3 cells,
565 an increase rather than a decrease in the ratio of PMEs/total P signal was observed by
566 *in vivo* $^{31}$P-MRS, and no significant difference in the tCho/water ratio was detected by
567 *in vivo* $^{1}$H-MRS pre vs. post MK-2206 treatment. Further investigations using *ex vivo*
568 MRS showed an increase in PE and a decrease in GPC and GPE in MK-2206 treated
569 subcutaneous PC3 tumour extracts when compared with vehicle controls. These
570 changes in choline and ethanolamine metabolites could explain the lack of change in
571 the *in vivo* MRS detected tCho/water signal as it consists of PC, PE, GPC and GPE,
572 and the increase in PMEs consisting of PC and PE.
573

Differences in phospholipid metabolism between PC3 cells in culture and in subcutaneous tumours derived from these cells have been previously reported and was attributed to the influence of the tumour microenvironment on choline and lipid metabolism (Mori *et al*, 2016). However, our MRS detected phospholipid changes observed in the colorectal HT29 subcutaneous tumours are consistent with our *in vitro* findings both in HT29 and PC3 cells and also in line with the previously published MRS changes using the AKT inhibitors perifosine and MK-2206 in breast cancer cells (Phyu *et al*, 2016; Su *et al*, 2012). We also did not observe any differences in the cellular or molecular effects of MK-2206 in both tumour models. We therefore questioned whether the difference in the phospholipid biomarker changes in the PC3 subcutaneous tumours was due to the location of the tumour, and whether growing PC3 tumours orthotopically would result in a different metabolic response to treatment with the AKT inhibitor MK-2206 compared to PC3 subcutaneous tumours. Orthotopic tumour models are more clinically relevant compared to subcutaneous tumours. A previous study showed images in real time, using green fluorescent protein (GFP) expression, of the very different tumour behaviour at the orthotopic and subcutaneous sites of human prostate cancer PC3 in athymic nude mice. The orthotopic tumour described had higher rates of vascularisation, migration, angiogenesis and metastasis compared to the subcutaneous tumour (Zhang *et al*, 2016). Indeed, inhibition of AKT signalling with MK-2206 in orthotopic PC3 tumours resulted in a significant reduction in the tCho/water ratio using *in vivo* $^{1}$H-MRS and this was due to a decrease in PC levels as shown in the MRS analysis of the tumour extracts. Similar to MK-2206 treated PC3 and HT29 cells, orthotopic PC3 tumours treated with MK-2206 also showed reduced alanine and increased glucose, suggesting an alteration in glucose metabolism. MK-2206 had no effect on tumour

bioenergetics, glutamine or glutathione metabolism, microvessel density, necrosis, proliferation or apoptosis. This shows that the difference in metabolic response between subcutaneous and orthotopic PC3 tumours could reflect the difference in tumour microenvironment at different tumour sites.

We have provided further evidence that *in vitro* inhibition of AKT is associated with changes in glucose, glutamine and choline metabolism both in prostate and colorectal cancer cell lines. We also demonstrated that the reduction in choline metabolites can be detected *in vivo* both in subcutaneous and the clinically relevant orthotopic prostate cancer tumours. A Phase I trial study published previously investigated the utility of $^{1}$H-MRS (amongst a number of functional imaging biomarkers) to monitor patient response to MK-2206 (Yap *et al*, 2014). Individual but not cohort $^{1}$H-MRS detected changes in tCho/water ratio have been reported. This was possibly due to insufficient target and pathway modulation as the ultimate maximum tolerated dose (MTD) was limited by Dose Limiting Toxicities (DLTs) of rash during dose escalation. The Phase I study also involved a very small population of patients. The authors suggested that functional imaging studies including total choline levels should be considered in phase II trials using a higher dose of MK-2206.

Taken together, our MRS-detected choline metabolites may have potential as non-invasive biomarkers for monitoring response to treatment with AKT inhibitors during Phase I/II clinical trials in selected cancer types.

**Additional Information:**

**Ethics approval**

All animal experiments were performed in accordance with local and national ethical review panel, the UK Home Office Animals (Scientific Procedures) Act 1986 and the United Kingdom Coordinating Committee on Cancer Research Guidelines for the Welfare of Animals in Experimental Neoplasia (Workman et al. *BJC* 2010)

**Availability of data and material**

All data generated or analysed during this study are included in this published article and its supplementary information files.

**Conflict of interest.**

The authors declare no conflict of interest.

**Funding**

This work is funded by Cancer Research UK and EPSRC Cancer Imaging Centre in association with the MRC and Department of Health (England) grant C1060/A10334 and C1060/A16464 for M.O.L, Y-L.C, N.M.S.A, A.C.W.T.F, R.P., S.P.R, J.K.R.B, and L.E.J. M.O.L is an Emeritus NIHR Senior Investigator. All authors acknowledge National Health Service funding to the NIHR Biomedical Research Centre.

**Authors' contributions**

NMSA and Y-LC wrote the manuscript text. NMSA, Y-LC, TAY and MOL conceived the study. NMSA, Y-LC, HT, LEJ, ACWTF, SG, RP and JKRB designed

and performed experiments. NMSA, Y-LC, ACWTF and SG analysed the data. NMSA, Y-LC, SPR, SAE and MOL contributed reagents/ materials/analysis tools. All authors reviewed the manuscript.

**Acknowledgements**

We thank Dr. Ian Titley and Mrs. G. Vijayaraghavan for their help with FACS analyses.

654 Supplementary information is available at the British Journal of Cancer's website

655

## References


Agarwal, E., Brattain, M. G., and Chowdhury, S. (2013). Cell survival and metastasis regulation by Akt signaling in colorectal cancer. Cell Signal *25*, 1711-1719.

Ahn, D. H., Li, J., Wei, L., Doyle, A., Marshall, J. L., Schaaf, L. J., Phelps, M. A., Villalona-Calero, M. A., and Bekaii-Saab, T. (2015). Results of an abbreviated phase-II study with the Akt Inhibitor MK-2206 in Patients with Advanced Biliary Cancer. Sci Rep *5*, 12122.

Al-Saffar, N. M., Jackson, L. E., Raynaud, F. I., Clarke, P. A., Ramírez de Molina, A., Lacal, J. C., Workman, P., and Leach, M. O. (2010). The Phosphoinositide 3-Kinase Inhibitor PI-103 Downregulates Choline Kinase {alpha} Leading to Phosphocholine and Total Choline Decrease Detected by Magnetic Resonance Spectroscopy. Cancer Res *70*, 5507-5517.

Al-Saffar, N. M., Marshall, L. V., Jackson, L. E., Balarajah, G., Eykyn, T. R., Agliano, A., Clarke, P. A., Jones, C., Workman, P., Pearson, A. D., and Leach, M. O. (2014). Lactate and choline metabolites detected in vitro by nuclear magnetic resonance spectroscopy are potential metabolic biomarkers for PI3K inhibition in pediatric glioblastoma. PLoS One *9*, e103835.

Beloueche-Babari, M., Chung, Y. L., Al-Saffar, N. M., Falck-Miniotis, M., and Leach, M. O. (2010). Metabolic assessment of the action of targeted cancer therapeutics using magnetic resonance spectroscopy. BrJCancer *102*, 1-7.

Beloueche-Babari, M., Jackson, L. E., Al-Saffar, N. M. S., Eccles, S. A., Raynaud, F. I., Workman, P., Leach, M. O., and Ronen, S. M. (2006). Identification of magnetic resonance detectable metabolic changes associated with inhibition of phosphoinositide 3-kinase signaling in human breast cancer cells. Molecular Cancer Therapeutics *5*, 187-196.

Beloueche-Babari, M., Workman, P., and Leach, M. O. (2011). Exploiting tumor metabolism for non-invasive imaging of the therapeutic activity of molecularly targeted anticancer agents. Cell Cycle *10*, 2883-2893.

Bosari, S., Lee, A. K., DeLellis, R. A., Wiley, B. D., Heatley, G. J., and Silverman, M. L. (1992). Microvessel quantitation and prognosis in invasive breast carcinoma. Hum Pathol *23*, 755-761.

Brown, J. S., and Banerji, U. (2017). Maximising the potential of AKT inhibitors as anti-cancer treatments. Pharmacol Ther *172*, 101-115.

Chaumeil, M. M., Ozawa, T., Park, I., Scott, K., James, C. D., Nelson, S. J., and Ronen, S. M. (2012). Hyperpolarized 13C MR spectroscopic imaging can be used to monitor Everolimus treatment in vivo in an orthotopic rodent model of glioblastoma. Neuroimage *59*, 193-201.

Chung, Y. L. (2017). Magnetic Resonance Spectroscopy (MRS)-Based Methods for Examining Cancer Metabolism in Response to Oncogenic Kinase Drug Treatment. Methods Mol Biol *1636*, 393-404.

Cory, J. G., and Cory, A. H. (2006). Critical roles of glutamine as nitrogen donors in purine and pyrimidine nucleotide synthesis: asparaginase treatment in childhood acute lymphoblastic leukemia. In Vivo *20*, 587-589.

Dai, B., Yoo, S. Y., Bartholomeusz, G., Graham, R. A., Majidi, M., Yan, S., Meng, J., Ji, L., Coombes, K., Minna, J. D. *et al* (2013). KEAP1-dependent synthetic lethality induced by AKT and TXNRD1 inhibitors in lung cancer. Cancer Res *73*, 5532-5543.

Esmaeili, M., Bathen, T. F., Engebraten, O., Maelandsmo, G. M., Gribbestad, I. S., and Moestue, S. A. (2014). Quantitative (31)P HR-MAS MR spectroscopy for detection of response to PI3K/mTOR inhibition in breast cancer xenografts. Magnetic

705 resonance in medicine : official journal of the Society of Magnetic Resonance in
706 Medicine / Society of Magnetic Resonance in Medicine *71*, 1973-1981.
707 Euceda, L. R., Hill, D. K., Stokke, E., Hatem, R., El Botty, R., Bieche, I., Marangoni,
708 E., Bathen, T. F., and Moestue, S. A. (2017). Metabolic Response to Everolimus in
709 Patient-Derived Triple-Negative Breast Cancer Xenografts. J Proteome Res *16*, 1868-
710 1879.
711 Gadian, D. G. (1995). The information available from NMR. In NMR and its
712 applications to living systems, (New York: Oxford University Press Inc.), pp. 29-64.
713 Hanahan, D., and Weinberg, R. A. (2011). Hallmarks of cancer: the next generation.
714 Cell *144*, 646-674.
715 Hensley, C. T., Wasti, A. T., and DeBerardinis, R. J. (2013). Glutamine and cancer:
716 cell biology, physiology, and clinical opportunities. J Clin Invest *123*, 3678-3684.
717 Iurlaro, R., Leon-Annicchiarico, C. L., and Munoz-Pinedo, C. (2014). Regulation of
718 cancer metabolism by oncogenes and tumor suppressors. Methods Enzymol *542*, 59-
719 80.
720 Khan, K. H., Yap, T. A., Yan, L., and Cunningham, D. (2013). Targeting the PI3K-
721 AKT-mTOR signaling network in cancer. Chin J Cancer *32*, 253-265.
722 Koul, D., Shen, R., Kim, Y. W., Kondo, Y., Lu, Y., Bankson, J., Ronen, S. M.,
723 Kirkpatrick, D. L., Powis, G., and Yung, W. K. (2010). Cellular and in vivo activity
724 of a novel PI3K inhibitor, PX-866, against human glioblastoma. NeuroOncol.
725 Lee, S. C., Marzec, M., Liu, X., Wehrli, S., Kantekure, K., Ragunath, P. N., Nelson,
726 D. S., Delikatny, E. J., Glickson, J. D., and Wasik, M. A. (2013). Decreased lactate
727 concentration and glycolytic enzyme expression reflect inhibition of mTOR signal
728 transduction pathway in B-cell lymphoma. NMR Biomed *26*, 106-114.

729 Lien, E. C., Lyssiotis, C. A., Juvekar, A., Hu, H., Asara, J. M., Cantley, L. C., and
730 Toker, A. (2016). Glutathione biosynthesis is a metabolic vulnerability in PI(3)K/Akt-
731 driven breast cancer. Nat Cell Biol *18*, 572-578.
732 Manning, B. D., and Toker, A. (2017). AKT/PKB Signaling: Navigating the Network.
733 Cell *169*, 381-405.
734 Moestue, S. A., Dam, C. G., Gorad, S. S., Kristian, A., Bofin, A., Maelandsmo, G.
735 M., Engebraten, O., Gribbestad, I. S., and Bjorkoy, G. (2013). Metabolic biomarkers
736 for response to PI3K inhibition in basal-like breast cancer. Breast Cancer Res *15*,
737 R16.
738 Moestue, S. A., Engebraaten, O., and Gribbestad, I. S. (2011). Metabolic effects of
739 signal transduction inhibition in cancer assessed by magnetic resonance spectroscopy.
740 Mol Oncol *5*, 224-241.
741 Mori, N., Wildes, F., Takagi, T., Glunde, K., and Bhujwalla, Z. M. (2016). The
742 Tumor Microenvironment Modulates Choline and Lipid Metabolism. Front Oncol *6*,
743 262.
744 Morse, D. L., Galons, J. P., Payne, C. M., Jennings, D. L., Day, S., Xia, G., and
745 Gillies, R. J. (2007). MRI-measured water mobility increases in response to
746 chemotherapy via multiple cell-death mechanisms. NMR Biomed *20*, 602-614.
747 Nitulescu, G. M., Margina, D., Juzenas, P., Peng, Q., Olaru, O. T., Saloustros, E.,
748 Fenga, C., Spandidos, D., Libra, M., and Tsatsakis, A. M. (2016). Akt inhibitors in
749 cancer treatment: The long journey from drug discovery to clinical use (Review). Int J
750 Oncol *48*, 869-885.
751 Pavlova, N. N., and Thompson, C. B. (2016). The Emerging Hallmarks of Cancer
752 Metabolism. Cell Metab *23*, 27-47.

753 Phyu, S. M., Tseng, C. C., Fleming, I. N., and Smith, T. A. (2016). Probing the
754 PI3K/Akt/mTor pathway using (31)P-NMR spectroscopy: routes to glycogen synthase
755 kinase 3. Sci Rep *6*, 36544.
756 Raynaud, F. I., Eccles, S., Clarke, P. A., Hayes, A., Nutley, B., Alix, S., Henley, A.,
757 Di-Stefano, F., Ahmad, Z., Guillard, S. *et al* (2007). Pharmacologic characterization
758 of a potent inhibitor of class I phosphatidylinositide 3-kinases. Cancer Research *67*,
759 5840-5850.
760 Serkova, N. J., and Eckhardt, S. G. (2016). Metabolic Imaging to Assess Treatment
761 Response to Cytotoxic and Cytostatic Agents. Front Oncol *6*, 152.
762 Shanware, N. P., Mullen, A. R., DeBerardinis, R. J., and Abraham, R. T. (2011).
763 Glutamine: pleiotropic roles in tumor growth and stress resistance. J Mol Med (Berl)
764 *89*, 229-236.
765 Sitter, B., Sonnewald, U., Spraul, M., Fjosne, H. E., and Gribbestad, I. S. (2002).
766 High-resolution magic angle spinning MRS of breast cancer tissue. NMR Biomed *15*,
767 327-337.
768 Su, J. S., Woods, S. M., and Ronen, S. M. (2012). Metabolic consequences of
769 treatment with AKT inhibitor perifosine in breast cancer cells. NMR Biomed *25*, 379-
770 388.
771 Tarrado-Castellarnau, M., de Atauri, P., and Cascante, M. (2016). Oncogenic
772 regulation of tumor metabolic reprogramming. Oncotarget *7*, 62726-62753.
773 Teng, F. F., Meng, X., Sun, X. D., and Yu, J. M. (2013). New strategy for monitoring
774 targeted therapy: molecular imaging. Int J Nanomedicine *8*, 3703-3713.
775 Toren, P., and Zoubeidi, A. (2014). Targeting the PI3K/Akt pathway in prostate
776 cancer: challenges and opportunities (review). Int J Oncol *45*, 1793-1801.

777 Tyagi, R. K., Azrad, A., Degani, H., and Salomon, Y. (1996). Simultaneous extraction
778 of cellular lipids and water-soluble metabolites: Evaluation by NMR spectroscopy.
779 Magnetic Resonance in Medicine *35*, 194-200.
780 Venkatesh, H. S., Chaumeil, M. M., Ward, C. S., Haas-Kogan, D. A., James, C. D.,
781 and Ronen, S. M. (2012). Reduced phosphocholine and hyperpolarized lactate provide
782 magnetic resonance biomarkers of PI3K/Akt/mTOR inhibition in glioblastoma.
783 NeuroOncol *14*, 315-325.
784 Workman, P., Aboagye, E. O., Balkwill, F., Balmain, A., Bruder, G., Chaplin, D. J.,
785 Double, J. A., Everitt, J., Farningham, D. A., Glennie, M. J. *et al* (2010). Guidelines
786 for the welfare and use of animals in cancer research. Br J Cancer *102*, 1555-1577.
787 Workman, P., Aboagye, E. O., Chung, Y. L., Griffiths, J. R., Hart, R., Leach, M. O.,
788 Maxwell, R. J., McSheehy, P. M., Price, P. M., and Zweit, J. (2006). Minimally
789 invasive pharmacokinetic and pharmacodynamic technologies in hypothesis-testing
790 clinical trials of innovative therapies. Journal Of The National Cancer Institute *98*,
791 580-598.
792 Yap, T. A., Smith, A. D., Ferraldeschi, R., Al-Lazikani, B., Workman, P., and de
793 Bono, J. S. (2016). Drug discovery in advanced prostate cancer: translating biology
794 into therapy. Nat Rev Drug Discov *15*, 699-718.
795 Yap, T. A., Yan, L., Patnaik, A., Fearen, I., Olmos, D., Papadopoulos, K., Baird, R.
796 D., Delgado, L., Taylor, A., Lupinacci, L. *et al* (2011). First-in-man clinical trial of
797 the oral pan-AKT inhibitor MK-2206 in patients with advanced solid tumors. J Clin
798 Oncol *29*, 4688-4695.
799 Yap, T. A., Yan, L., Patnaik, A., Tunariu, N., Biondo, A., Fearen, I., Papadopoulos,
800 K. P., Olmos, D., Baird, R., Delgado, L. *et al* (2014). Interrogating two schedules of
801 the AKT inhibitor MK-2206 in patients with advanced solid tumors incorporating

novel pharmacodynamic and functional imaging biomarkers. Clin Cancer Res *20*, 5672-5685.

Zhang, Y., Chen, X., Gueydan, C., and Han, J. (2018). Plasma membrane changes during programmed cell deaths. Cell Res *28*, 9-21.

Zhang, Y., Toneri, M., Ma, H., Yang, Z., Bouvet, M., Goto, Y., Seki, N., and Hoffman, R. M. (2016). Real-Time GFP Intravital Imaging of the Differences in Cellular and Angiogenic Behavior of Subcutaneous and Orthotopic Nude-Mouse Models of Human PC-3 Prostate Cancer. J Cell Biochem *117*, 2546-2551.

## Figure Legends

**Figure 1. Molecular and metabolic changes caused by treatment with MK-2206 in PC3 prostate cancer cells.** (**A**) Representative immunoblots showing changes in molecular markers demonstrating AKT inhibition and induction of apoptosis as evidenced by cleaved PARP. β-Actin is used as a loading control. (**B**) Flow cytometry analysis histograms showing cell cycle distribution of cells with vehicle treatment (DMSO, control), or following treatment with MK-2206 ($5xGI_{50}$) at 24 h post treatment, $P < 0.002$ for G1&S phases. (**C**) Representative *in vitro* $^{31}$P-MR spectra (left) and expansion of $^{1}$H-MR spectra region (1.3-3.3 ppm; right) showing choline–containing metabolites, Cr/PCr, lactate (Lac) and amino acids (Ala = alanine; Glu = glutamate; Gln = glutamine; GSH = glutathione). A summary of $^{1}$H-MRS metabolic changes caused by MK-2206 treatment ($5xGI_{50}$, 24 h) of PC3 prostate cancer cells: (**D**) Choline-containing metabolites. (**E**) Amino acids, Cr/PCr and glycolytic intermediates. Results are expressed as %T/C and presented as mean ± SD, $n \geq 5$. Statistically significant differences from the control $^{*}P \leq 0.05$, $^{**}P \leq 0.01$; $^{***}P \leq 0.001$.

**Figure 2. Tumour volume and histological changes in subcutaneous tumours following MK-2206 treatment.** Percentage change in HT29 (**A**) and subcutaneous PC3 (**B**) tumour volumes (relative to Day 1) following 2 doses (Day 1 and 3) of 120 mg/kg of MK-2206 on alternate days via p.o. (n = 10) or vehicle alone (10% DMSO in saline), minimum n = 10. Data are expressed as mean ± SEM, ****$P < 0.0001$. (**C**) Immunohistochemistry of Ki67, caspase-3 and CD31 expressions (brown staining) in

835 vehicle-treated control (left column) and MK-2206 treated (right column)
836 subcutaneous PC3 xenografts (right column). Magnification x 200.
837

**Table 1. Analysis of $^{31}$P-MRS-detected metabolic changes following inhibition with MK-2206 in:**

| | PC3 | | | | | | | |
|---|---|---|---|---|---|---|---|---|
| | 6 h ($5xGI_{50}$) | *P* | 12 h ($5xGI_{50}$) | *P* | 24 h ($5xGI_{50}$) | *P* | 24 h ($3xGI_{50}$) | *P* |
| PE | 62 ± 16 | 0.008 | 47 ± 11 | 0.001 | 23 ± 16 | 0.0001 | 43 ± 26 | 0.01 |
| PC | 74 ± 14 | 0.02 | 78 ± 11 | 0.02 | 69 ± 13 | 0.001 | 71 ± 5 | 0.0004 |
| GPE | 66 ± 34 | ns | 50 ± 12 | 0.001 | 320 ± 104 | 0.005 | 153 ± 40 | ns |
| GPC | 32 ± 16 | 0.001 | 36 ± 11 | 0.0003 | 225 ± 63 | 0.007 | 121 ± 27 | ns |
| PCr | 74 ± 28 | ns | 54 ± 31 | 0.04 | 38 ± 24 | 0.007 | 46 ± 24 | 0.01 |
| NTP | 63 ± 17 | 0.01 | 56 ± 12 | 0.002 | 68 ± 18 | 0.005 | 82 ± 11 | 0.03 |

Data are expressed as %T/C and presented as the mean ± SD, n ≥ 4.
Two-tailed unpaired *t* test was used to compare results in treated cells to controls within the same time-point.

| | HT29 | |
|---|---|---|
| | 24 h ($5xGI_{50}$) | *P* |
| PE | 60 ± 9 | 0.001 |
| PC | 67 ± 6 | 0.0001 |
| GPE | 132 ± 26 | 0.04 |
| GPC | 169 ± 31 | 0.004 |
| PCr | 59 ± 8 | 0.0001 |
| NTP | 89 ± 7 | 0.02 |

**Table 2: *In vivo* and *ex vivo* $^{1}$H- and $^{31}$P-MRS metabolic analysis of HT29 subcutaneous tumours and extracts following MK-2206 treatment.**

***In vivo* $^{1}$H-MRS of subcutaneous HT29 xenografts**

| | Vehicle-Control (n=5) | | MK-2206 (n=5) | |
|---|---|---|---|---|
| | Pre- | Post- | Pre | Post |
| Corrected tCho/water ratio x $10^{-3}$ | 8.05 ± 1.11 | 6.25 ± 1.84 | 9.22 ± 1.42 | 4.33 ±1.03 |
| | $P = 0.31$ | | $^{*}P = 0.04$ | |

*Statistically significant when compared the pre-MK-2206 treatment values with post-treatment. Two-tailed paired *t* test was used and data are expressed as mean±sem.

***Ex vivo* $^{1}$H- and $^{31}$P-MRS of subcutaneous HT29 tumour extracts**

| | Vehicle-Control | MK-2206 | *p* |
|---|---|---|---|
| PE | 1.27 ± 0.10 | 1.28 ± 0.11 | 0.96 |
| PC | 1.95 ± 0.12 | 1.60 ± 0.09 | 0.04* |
| GPE | 1.21 ± 0.14 | 0.87 ± 0.07 | 0.03* |
| GPC | 2.51 ± 0.13 | 1.94 ± 0.18 | 0.04* |
| Lactate | 5.81 ± 0.58 | 7.78 ± 0.92 | 0.10 |
| Alanine | 1.49 ± 0.15 | 1.27 ± 0.08 | 0.25 |
| Glucose | 0.79 ± 0.10 | 0.70 ± 0.13 | 0.61 |
| Glutamine | 1.01 ± 0.06 | 0.72 ± 0.02 | 0.002* |
| Glutamate | 2.67 ± 0.23 | 1.56 ± 0.30 | 0.02* |
| Aspartate | 0.35 ± 0.04 | 0.20 ± 0.05 | 0.05* |
| Glycine | 0.67 ± 0.11 | 0.37 ± 0.06 | 0.04* |
| Glutathione | 1.30 ± 0.11 | 0.85 ± 0.08 | 0.007* |
| Creatine | 3.82 ± 0.21 | 2.87 ± 0.19 | 0.008* |
| Phosphocreatine | 1.20 ± 0.08 | 0.74 ± 0.08 | 0.004* |
| ATP+ADP | 1.38 ± 0.08 | 1.07 ± 0.07 | 0.02* |

Data are expressed as µmol/g wet weight and presented as the mean±sem, $n \geq 5$ in each group. Two-tailed unpaired *t* test was used to compare MK2206-treated tumour extracts with vehicle-treated controls and $^{*}P \leq 0.05$ is considered significant.

**Table 3: *In vivo* and *ex vivo* $^{1}$H- and $^{31}$P-MRS metabolic analysis of subcutaneous PC3 tumours and extracts following MK-2206 treatment.**

***In vivo* $^{1}$H- and $^{31}$P-MRS of subcutaneous PC3 tumours**

| | Vehicle-Control | | MK-2206 | |
|---|---|---|---|---|
| | Pre- | Post- | Pre- | Post- |
| Corrected tCho/water ratio x$10^{-3}$ (n = 4 in each group) | 3.63 ± 0.38 | 3.80 ± 0.64 | 3.26 ± 0.26 | 3.61 ± 0.17 |
| | $P = 0.66$ | | $P = 0.31$ | |
| PME/total P ratio (n = 5 in each group) | 0.11 ± 0.01 | 0.12 ± 0.01 | 0.14 ± 0.01 | 0.17 ± 0.02 |
| | $P = 0.50$ | | $^{*}P = 0.02$ | |

*Statistically significant when compared the pre-MK-2206 treatment values with post-treatment. Two-tailed paired *t* test was used and data are expressed as mean±sem. PME – phosphomonoesters, total P – total phorphorus signal.

***Ex vivo* $^{1}$H- and $^{31}$P-MRS of subcutaneous PC3 tumour extracts**

| | Vehicle-Control | MK-2206 | *p* |
|---|---|---|---|
| PE | 1.03 ± 0.10 | 1.45 ± 0.13 | 0.03* |
| PC | 1.53 ± 0.05 | 1.60 ± 0.20 | 0.75 |
| GPE | 0.44 ± 0.03 | 0.28 ± 0.04 | 0.02* |
| GPC | 1.54 ± 0.14 | 0.94 ± 0.19 | 0.04* |
| Lactate | 9.34 ± 0.85 | 7.14 ± 0.44 | 0.04* |
| Alanine | 1.39 ± 0.13 | 1.49 ± 0.23 | 0.74 |
| Glucose | 0.45 ± 0.06 | 0.41 ± 0.03 | 0.48 |
| Glutamine | 1.20 ± 0.16 | 2.74 ± 0.48 | 0.02* |
| Glutamate | 3.64 ± 0.41 | 3.02 ± 0.37 | 0.28 |
| Glycine | 1.21 ± 0.18 | 1.39 ± 0.16 | 0.48 |
| Glutathione | 1.53 ± 0.15 | 1.46 ± 0.12 | 0.74 |
| Creatine | 1.08 ± 0.09 | 1.38 ± 0.24 | 0.32 |
| Phosphocreatine | 0.39 ± 0.05 | 0.53 ± 0.05 | 0.08 |
| ATP+ADP | 0.84 ± 0.05 | 0.89 ± 0.07 | 0.63 |

Data are expressed as µmol/g wet weight and presented as the mean±sem, n ≥ 5 in each group. Two-tailed unpaired *t* test was used to compare MK2206-treated tumour extracts with vehicle-treated controls and $^{*}P \leq 0.05$ is considered significant. Aspartate was not detected.

**Table 4: *In vivo* and *ex vivo* $^{1}$H- and $^{31}$P-MRS metabolic analysis of orthotopic PC3 tumours and extracts following MK-2206 treatment.**

| ***In vivo* $^{1}$H-MRS of orthotopic PC3 tumours** | | | | |
|---|---|---|---|---|
| | **Vehicle-Control (n=3)** | | **MK-2206 (n=5)** | |
| | **Pre-** | **Post-** | **Pre** | **Post** |
| Corrected tCho/water ratio x$10^{-3}$ | 5.11 ± 0.68 | 4.25 ± 0.47 | 5.03 ± 0.69 | 3.92 ± 0.56 |
| | *P* = 0.36 | | **P* = 0.02 | |
| *Statistically significant when compared the pre-MK-2206 treatment values with post-treatment. Two-tailed paired *t* test was used and data are expressed as mean±sem. | | | | |

| ***Ex vivo* $^{1}$H- and $^{31}$P-MRS of orthotopic PC3 tumour extracts** | | | |
|---|---|---|---|
| | **Vehicle-Control** | **MK-2206** | ***P*** |
| PE | 1.58 ± 0.18 | 1.20 ± 0.13 | 0.14 |
| PC | 1.80 ± 0.06 | 1.47 ± 0.06 | 0.003* |
| GPE | 0.46 ± 0.03 | 0.45 ± 0.05 | 0.95 |
| GPC | 1.79 ± 0.35 | 2.16 ± 0.17 | 0.40 |
| Lactate | 5.32 ± 0.65 | 3.96 ± 0.50 | 0.14 |
| Alanine | 1.09 ± 0.09 | 0.78 ± 0.07 | 0.03* |
| Glucose | 0.33 ± 0.04 | 0.79 ± 0.15 | 0.009* |
| Glutamine | 1.28 ± 0.16 | 0.97 ± 0.13 | 0.18 |
| Glutamate | 3.10 ± 0.25 | 2.50 ± 0.16 | 0.08 |
| Aspartate | 0.10 ± 0.02 | 0.08 ± 0.01 | 0.39 |
| Glycine | 1.06 ± 0.05 | 1.01 ± 0.14 | 0.76 |
| Glutathione | 1.59 ± 0.32 | 1.07 ± 0.09 | 0.19 |
| Creatine | 1.30 ± 0.16 | 1.17 ± 0.53 | 0.26 |
| Phosphocreatine | 0.36 ± 0.10 | 0.28 ± 0.04 | 0.50 |
| ATP+ADP | 0.98 ± 0.08 | 0.89 ± 0.08 | 0.46 |
| Data are expressed as µmol/g wet weight and presented as the mean±sem, n ≥ 5 in each group. Two-tailed unpaired *t* test was used to compare MK2206-treated tumour extracts with vehicle-treated controls and $^{*}P \leq 0.05$ is considered significant. | | | |

**Figure 1**

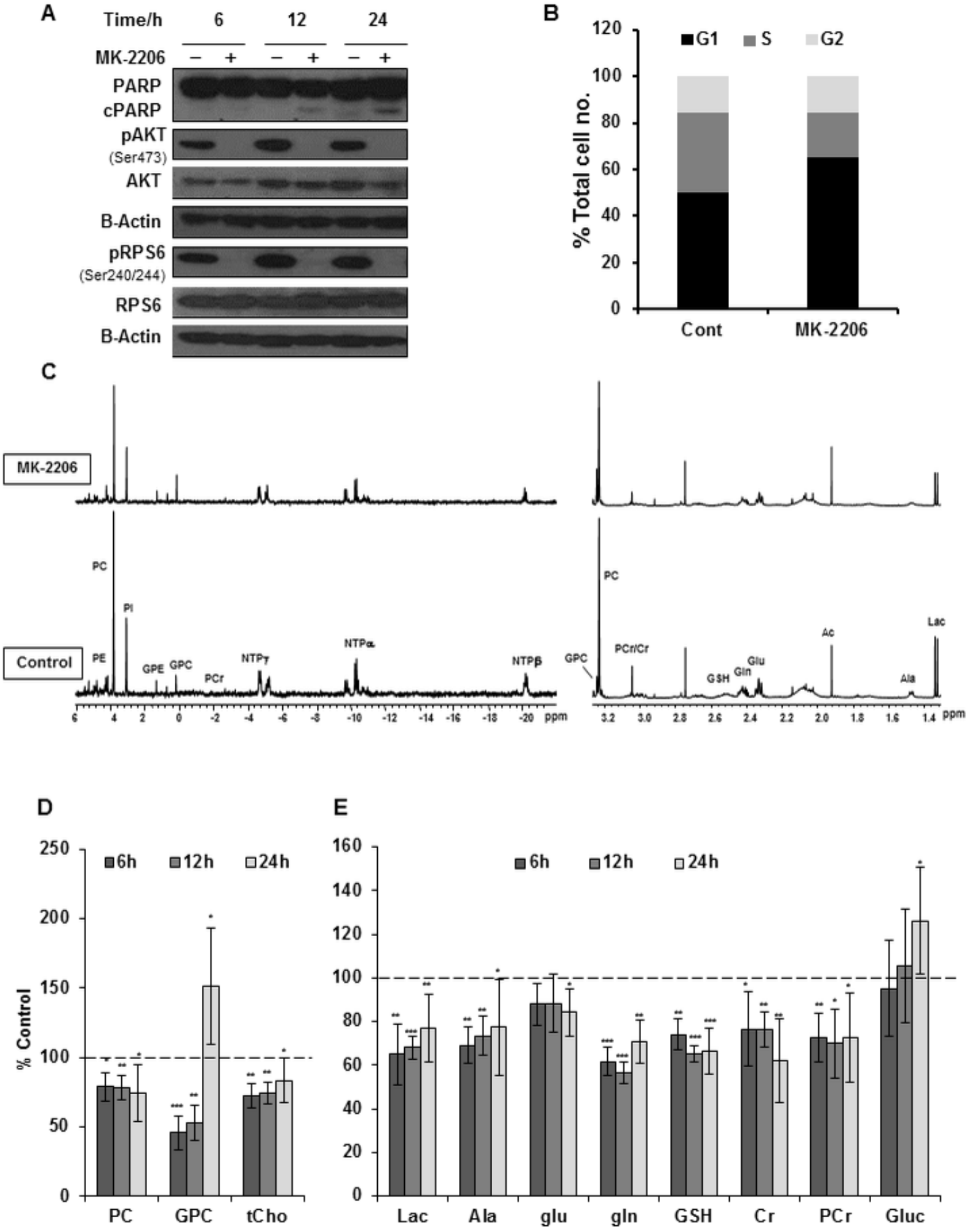
A
Time/h
6
12
24
MK-2206
– + – + – +
PARP
cPARP
pAKT
(Ser473)
AKT
B-Actin
pRPS6
(Ser240/244)
RPS6
B-Actin
B
G1
S
G2
% Total cell no.
120
100
80
60
40
20
0
Cont
MK-2206
C
MK-2206
Control
PC
PI
PE
GPE
GPC
PCr
NTPγ
NTPα
NTPβ
GPC
PC
PCr/Cr
GSH
Gln
Glu
Ac
Lac
Ala
6 4 2 0 -2 -4 -6 -8 -10 -12 -14 -16 -18 -20 ppm
3.2 3.0 2.8 2.6 2.4 2.2 2.0 1.8 1.6 1.4 ppm
D
% Control
250
200
150
100
50
0
6h
12h
24h
PC
GPC
tCho
E
160
140
120
100
80
60
40
20
0
6h
12h
24h
Lac
Ala
glu
gln
GSH
Cr
PCr
Gluc

# Figure 2

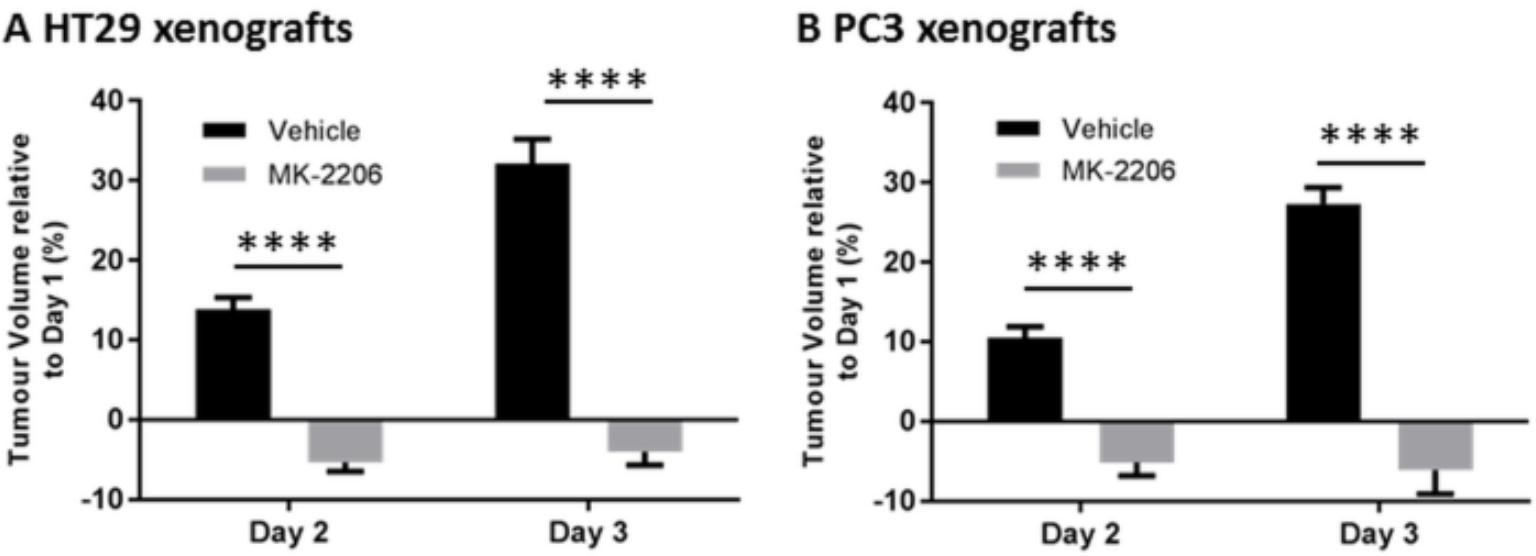
A HT29 xenografts
B PC3 xenografts
Tumour Volume relative to Day 1 (%)
Vehicle
MK-2206
****
Day 2
Day 3
40
30
20
10
0
-10

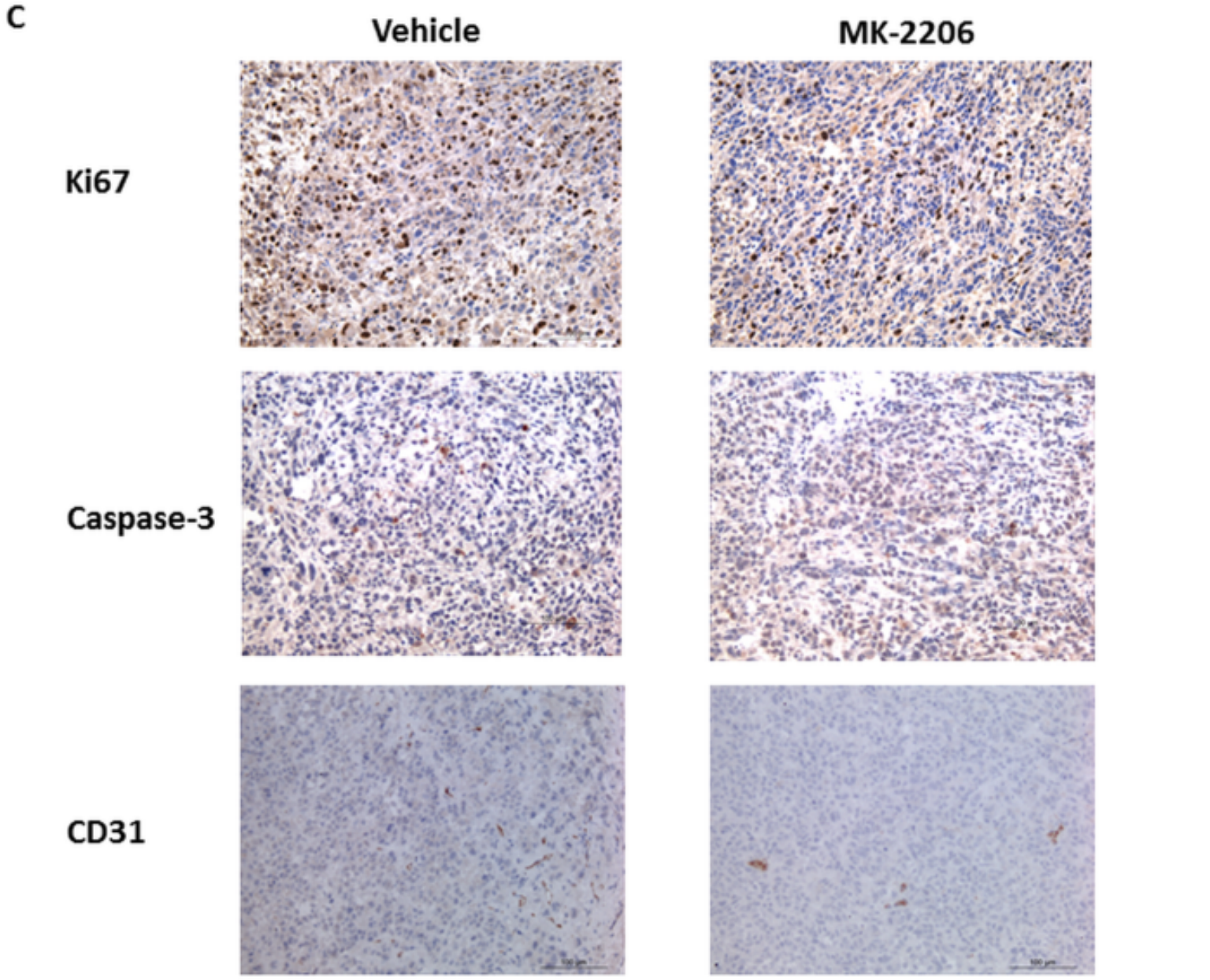
C
Vehicle
MK-2206
Ki67
Caspase-3
CD31